J Mol Model (2013) 19:4585–4590
DOI 10.1007/s00894-013-1967-9

ORIGINAL PAPER

Density functional study of bare gold clusters: the ten-vertex neutral system

Menyhárt B. Sárosi · Petronela M. Petrar · R. Bruce King

Received: 3 July 2013 / Accepted: 29 July 2013 / Published online: 22 August 2013

Abstract Four novel Au_{10} structures have been located by means of density functional methods and their geometry and electronic structure are discussed. Furthermore, the behavior of less extensive basis sets in conjunction with the B3PW91 functional is compared to a highly accurate and more extensive energy-consistent scalar-relativistic pseudopotential and basis set for neutral ten-vertex gold clusters. The values obtained for several structural parameters for known and novel optimized Au_{10} systems are discussed.

Keywords Basis set evaluation · Density functional theory · Gold clusters

Introduction

The neutral Au_{10} system has been the focus of numerous theoretical studies [1–4]. The ten-vertex neutral system is of particular importance since the transition from two dimensional (2D) to three dimensional (3D) cluster geometries has been suggested to occur at an atom number of ten for neutral gold clusters [5]. Further evidence for a 2D→3D transition at Au_{10} has been provided in a recent density functional theory (DFT) study showing a coexistence of both 2D and 3D Au_{10} structures, while Au_9 and Au_{11} clusters have been predicted to prefer 2D and 3D structures, respectively [6]. It has been noted that the exact cluster size at which the 2D→3D transition occurs depends on the chosen theoretical method [4, 7, 8]. However, smaller gold clusters are known to favor planar structures owing to relativistic effects [9]. Furthermore, MP2 or CCSD(T) with small basis sets can wrongly favor 3D structures over the actual 2D minima, when compared with DFT and experimental observations [10]. In this study, we present novel neutral Au_{10} structures identified with the help of DFT methods. The geometries and electronic structures of the novel Au_{10} clusters are discussed. Additionally, we also present a brief study of the basis set effects in the case of neutral Au_{10} clusters. The most widely used method in heavy element calculations is the relativistic pseudopotential approximation. However, the use of extensive relativistic basis sets can be highly demanding in computer time and thus prohibitive for certain types of calculations. Nevertheless, qualitatively good results can be obtained with smaller relativistic basis sets [1]. Thus, the structural data and electronic properties obtained using less extensive basis sets of known or novel optimized Au_{10} structures are assessed against the same parameters obtained using a highly accurate and more extensive energy-consistent scalar-relativistic pseudopotential and basis set.

Computational details

All calculations were carried out with the Gaussian09 program package [11] using the B3PW91 density functional [12–16] which has been previously reported to give results in agreement with more precise coupled-cluster calculations [17, 18]. An augmented triple-zeta quality basis set in combination with a fully relativistic effective core potential (ECP) was chosen for the reference calculations [19, 20]. This basis set and ECP will be denoted herein as RECP. The starting geometries were either taken from the literature (top row on Scheme 1) [1–3],

Electronic supplementary material The online version of this article (doi:10.1007/s00894-013-1967-9) contains supplementary material, which is available to authorized users.

M. B. Sárosi · P. M. Petrar
Department of Chemistry, Faculty of Chemistry and Chemical Engineering, Babeş-Bolyai University, M. Kogălniceanu 1, RO-400084 Cluj-Napoca, Romania

R. B. King (✉)
Department of Chemistry, University of Georgia, Athens, Georgia 30602
e-mail: rbking@chem.uga.edu

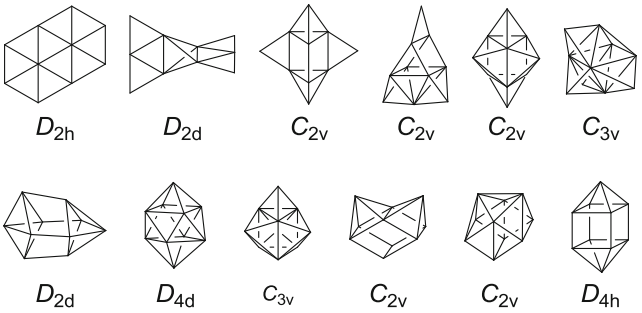

Scheme 1 Starting Au_{10} geometries

or derived from ten-vertex germanium clusters of high symmetry (bottom row on Scheme 1) [21]. The former starting geometries were chosen to provide well established reference structures. The later starting geometries were chosen in order to locate novel minima on the potential energy surface of the neutral Au_{10} system.

In order to study the basis set effects, calculations using smaller basis sets were carried out with the same options as for the B3PW91/RECP level of theory. The first set of calculations used the def2–TZVPD basis set and ECP [22, 23]. The second set of calculations were carried out with the LANL2TZ(f) basis set and ECP [24–26]. These two basis set and ECP combinations were obtained from the EMSL basis set library [27, 28]. Optimizations with all three methods were started from the same initial input geometries in the singlet state. All of the imaginary frequencies identified with the B3PW91/RECP method were followed until the optimizations arrived at a local minimum structure. The imaginary frequencies identified with the remaining two less extensive basis sets were followed only until the optimizations reached the same geometries as the B3PW91/RECP calculations. Besides Au–Au bonding distances, Au–Au–Au angles and HOMO–LUMO gaps, the atomic polar tensor (APT) atomic charges and vibrational frequency shifts are also considered.

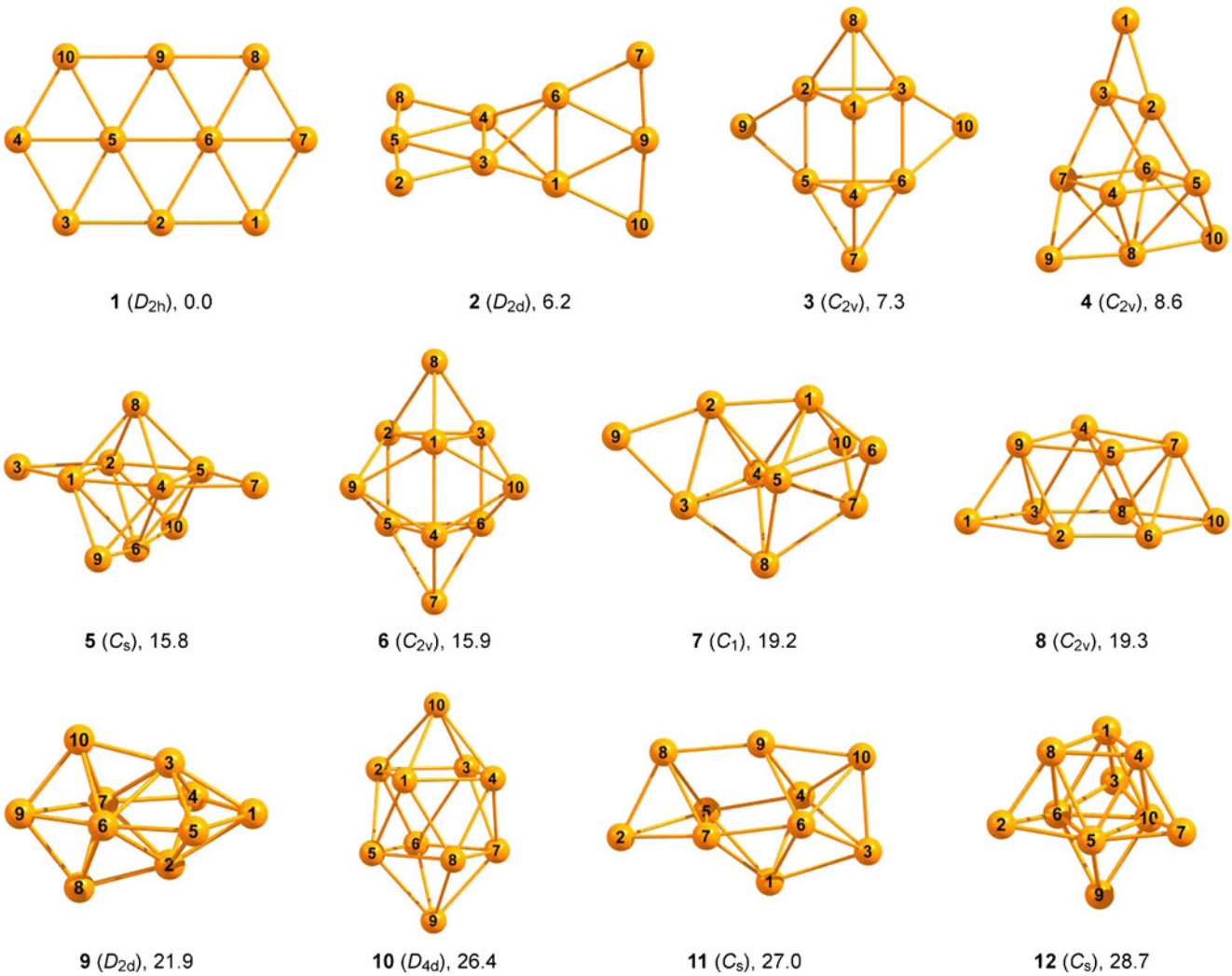

Fig. 1 B3PW91/RECP optimized Au_{10} geometries ordered according to increasing relative energy values (kcal mol^{-1}, including zero point vibrational energies)

Furthermore, differences in the cohesive energy (E_{coh}) are also addressed, where E_{coh} for ten-vertex gold clusters is defined as $E_{coh}=[10\cdot E(Au)-E(Au_{10})]/10$, with $E(Au)$ denoting the calculated total electronic energy of the gold atom [1].

Results and discussion

Novel Au_{10} structures

The B3PW91/RECP method predicts a planar Au_{10} ground state geometry (**1** on Fig. 1), followed closely by the four geometries obtained from the literature (**2**, **3**, **4** and **6** on Fig. 1) [1–4]. Structure **12** has also been reported earlier [3], but not with DFT methods. As stated above, these starting geometries were chosen to provide well established reference structures. Our results reproduce with excellent agreement the predictions from previous calculations [1, 2]. The B3PW91/RECP method gives the same relative energy ordering for the previously reported structures and the atomic charge distribution patterns are also in agreement with the literature data [1, 2]. The B3PW91/RECP HOMO–LUMO gaps, nearest-neighbor distances and cohesive energies of the two lowest lying Au_{10} clusters also show very tight correlation with previously calculated data [1]. The sites for electrophilic and nucleophilic attack suggested by the shape of the frontier molecular orbitals of **1**, **4** and **6** calculated at the B3PW91/RECP level are the same as the sites reported using a different DFT method (see the Electronic supplementary material) [2].

Two of the optimizations started from the germanium cluster geometries converged to structures already reported in the literature [3]. The 3D structure **9** has been identified as the ground state and the 2D structure **1** is a higher lying Au_{10} isomer according to David et al. [3]. For the discussion of the differences between the MP2 and DFT methods, see ref [4]. Structure **5** has been described by the same authors as a higher energy 3D structure [3].

The remaining optimizations started from the germanium cluster geometries converged to the novel neutral Au_{10} structures **7**, **8**, **10** and **11** which, to our knowledge, have not been reported in the literature so far. Structure **10** resembles the geometry and has the same symmetry as the dicationic Au_{10}^{2+} ground state structure proposed by Chen and co-workers [29]. However, recent studies showed that the Au_{10}^{2+} system has a tetrahedral cluster as the ground state [30, 31].

All of the above presented optimized structures are minima without any imaginary vibrational frequencies (see the Electronic supplementary material). With the increase in relative energy, a decreasing trend in the HOMO–LUMO gap of the Au_{10} clusters can be observed (Fig. 3), confirming that a large HOMO–LUMO gap is characteristic for stable clusters [32].

The novel structure **7** can be obtained by displacing one of the apical atoms of structure **9**. In this manner, a small planar segment formed by the Au2, Au3 and Au9 atoms is introduced. The smallest and largest gold-gold distances in **7** are 2.634 Å (Au3–Au9) and 2.952 Å (between Au4 and Au5), respectively. The frontier molecular orbitals of **7** are shown on Fig. 2. The HOMO of **7** is mainly made of the s atomic orbital on Au9 and an Au1–Au2 bonding orbital, indicating the preferred sites for an electrophilic attack. Mainly the contributions from Au3 and Au7 atomic orbitals make up the LUMO of **7** and provide the preferred sites for a nucleophilic attack. Structure **8** is constructed from an inner trigonal prism symmetrically capped on two vicinal faces to form two

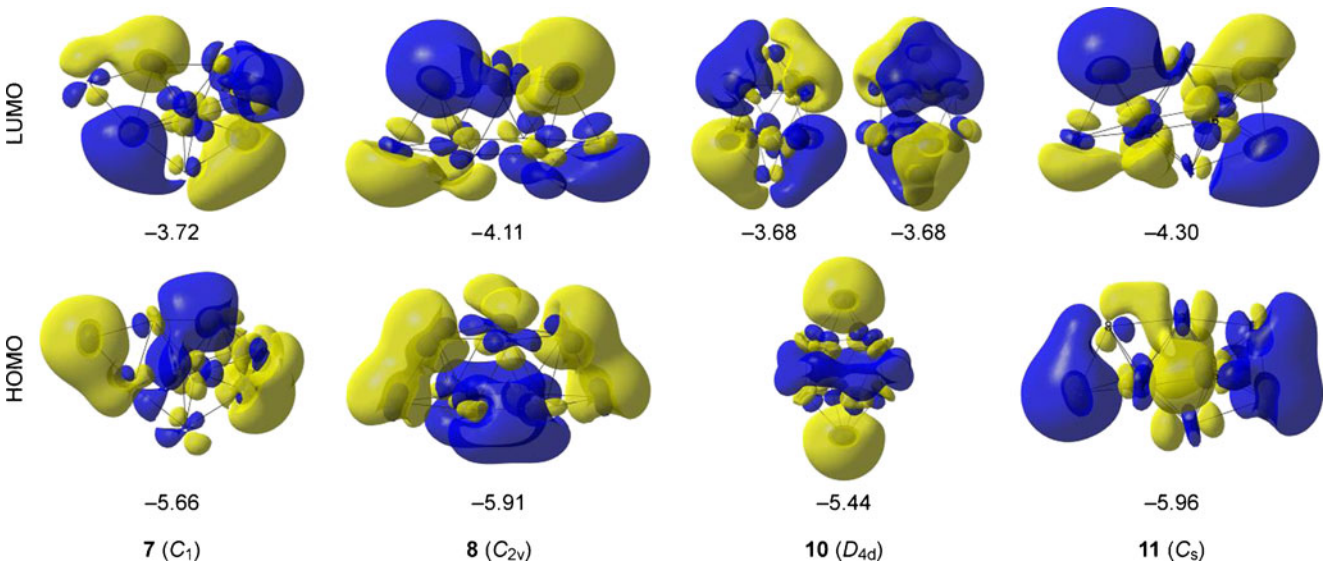

Fig. 2 Frontier molecular orbitals and corresponding orbital energies of the novel Au_{10} structures calculated at the B3PW91/RECP level of theory (energies in eV, isovalue = 0.02, see Fig. 1 for atom numbering)

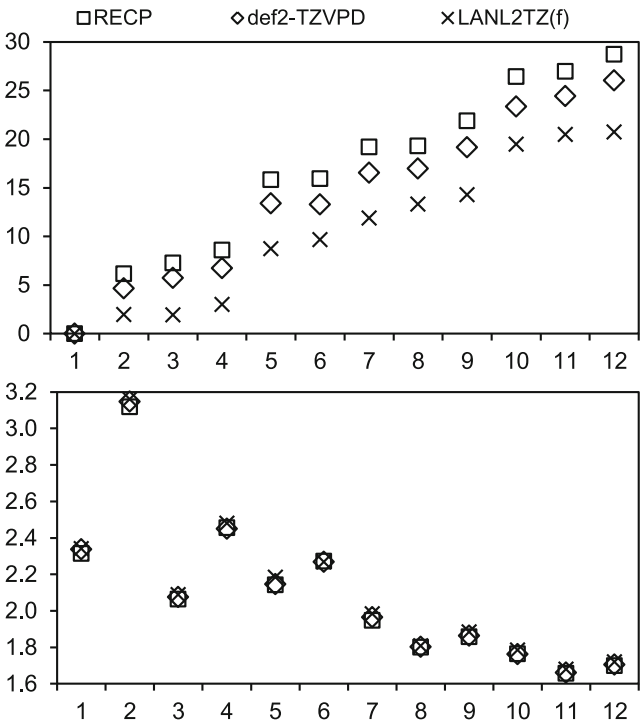

Fig. 3 Relative energies (top, including zero point vibrational energies, kcal mol^{-1}) and HOMO–LUMO gaps (bottom, eV) of the optimized Au_{10} structures

additional rectangular pyramidal cavities and two tetrahedral cavities (Fig. 1). The Au2–Au6 and Au3–Au8 bonding orbitals contribute mainly to the HOMO of **8**. The LUMO of **8** is mainly distributed around the Au9 and Au7 atoms. Thus, while electrophiles will attack **8** from the "top", nucleophiles will prefer an attack from the "bottom" of **8**. Structure **10** is a bicapped tetragonal antiprism with high symmetry. Accordingly, the frontier orbitals of **10** are also symmetric. The HOMO of **10** is mainly composed of the Au9 and Au10 s atomic orbitals. Thus, the capping atoms of **10** are the most vulnerable toward an electrophilic attack. On the other hand, the preferred sites for a nucleophilic attack are located on the gold atoms forming the tetragonal antiprism, as indicated by the doubly degenerate LUMO of **10**. The HOMO of **11** is mainly made of an s atomic orbital on Au2 and the main contributions to the LUMO of **11** come from the Au8 and Au3 atomic orbitals.

Basis set effects

The B3PW91/def2–TZVPD optimizations converged in all cases to the same global and local geometries with the same symmetry as the B3PW91/RECP calculations. The B3PW91/def2–TZVPD relative energies of the optimized structures are almost identical with the relative energies predicted at the B3PW91/RECP level of theory (Fig. 3). Furthermore, the mean unsigned error (MUE) with respect to the reference basis set for structural and electronic properties of the B3PW91/def2–TZVPD level of theory are negligible (Table 1). The B3PW91/def2–TZVPD method leads to insignificant positive differences in the Au–Au distances and Au–Au–Au angles, the former of only 0.02 Å and the latter of only 0.13º.

The HOMO–LUMO gaps are insignificantly overestimated by the B3PW91/def2–TZVPD method, by only 0.01 eV. Furthermore, the frontier molecular orbitals of **1**, **4** and **6** calculated at the B3PW91/def2–TZVPD level of theory have the same shapes as the frontier molecular orbitals calculated with the reference method and the individual orbital energies are practically the same (see the Electronic supplementary material). The electronic structures of the remaining Au_{10} isomers calculated at the B3PW91/def2–TZVPD level are also in perfect agreement with the predictions of the reference method.

The cohesion energy E_{coh} is underestimated by less than 2 kcal mol^{-1} when using the def2–TZVPD basis set and ECP. The B3PW91/def2–TZVPD APT charges, dipole moments and the vibrational frequencies are also in excellent agreement with the corresponding values predicted by the reference method. Thus, the def2–TZVPD basis set and ECP gives relative energies, geometrical parameters and electronic structure data in very good agreement with the reference basis set, at least in combination with the B3PW91 density functional.

The B3PW91/LANL2TZ(f) optimizations, in almost all cases, converged to the same global and local minimum geometries as the B3PW91/RECP calculations. The exceptions are the structures **6**, **8** and **10**. These geometries were identified as local minima with both the reference B3PW91/RECP calculations and the B3PW91/def2–TZVPD method. However, the structures **6**, **8** and **10** possess one or more small imaginary vibrational frequencies at the B3PW91/LANL2TZ(f) level of theory (see the Electronic supplementary material). In the case of **6** and **8**, these small imaginary frequencies are removed after reoptimizing the structures with only slight geometric distortions (RMSD of 0.12 and 0.06, respectively) [33]. Following the largest imaginary frequency of **10** however leads to a more distorted first order saddle point

Table 1 Mean unsigned errors (MUE) compared to the B3PW91/RECP method

	def2-TZVPD	LANL2TZ(f)
Au–Au distances [Å]	0.02	0.01
Au–Au–Au angles [º]	0.13	0.20
HOMO–LUMO gap [eV]	0.01	0.02
APT atomic charges	0.01	0.01
Frequencies [cm^{-1}]	1.95	1.56
E_{coh} [kcal mol^{-1}]	1.54	0.36
Dipole moment	0.01	0.03

(RMSD = 0.69, see Electronic supplementary material). Furthermore, the B3PW91/LANL2TZ(f) relative energies of the optimized structures are significantly lower than the relative energies predicted at the reference level of theory (Fig. 3). For instance, the structures **2** and **3** are predicted to be isoenergetic at the B3PW91/LANL2TZ(f) level of theory while the same two structures are separated in terms of relative energy by both the RECP and the def2–TZVPD calculations. Another inconsistency is observed in the case of structures **5** and **6**. These two structures are predicted to lie at different relative energy values by the B3PW91/LANL2TZ(f) level of theory. However, the reference method and the B3PW91/def2–TZVPD level of theory predict the structures **5** and **6** to be practically isoenergetic. Furthermore, the ZPE corrected B3PW91/LANL2TZ(f) relative energies deviate more from the reference results than the ZPE corrected relative energies obtained at the B3PW91/def2–TZVPD level of theory (Fig. 3). In spite of all these differences in relative energies between B3PW91/LANL2TZ(f) and the other two methods, the B3PW91/LANL2TZ(f) MUE values for structural parameters are also negligible (Table 1). The B3PW91/LANL2TZ(f) method leads to practically the same values as the reference method for the Au–Au distances and Au–Au–Au angles. The differences are only 0.01 Å for the former and 0.20º for the latter.

The HOMO–LUMO gaps are insignificantly overestimated by the B3PW91/LANL2TZ(f) method, by only 0.01 eV. Furthermore, the frontier molecular orbitals of **1**, **4** and **6** calculated at the B3PW91/LANL2TZ(f) level of theory have the same shapes as the frontier molecular orbitals calculated with the reference method. However, the individual orbital energies are overestimated (see the Electronic supplementary material). Nevertheless, the HOMO–LUMO gaps calculated at the B3PW91/LANL2TZ(f) level are in good agreement with the HOMO–LUMO gaps determined at the reference level of theory.

The cohesion energy E_{coh} is underestimated by less than 1 kcal mol^{-1} using the LANL2TZ(f) basis set and ECP. The B3PW91/LANL2TZ(f) APT charges, dipole moments and the vibrational frequencies are also in good agreement with the corresponding values predicted by the reference method. Thus, the B3PW91/LANL2TZ(f) method gives geometrical parameters, orbital energies, APT charge distributions and other properties in good agreement with the reference calculations. However, using the LANL2TZ(f) basis set leads to significantly lower relative energy values and sometimes different relative energy orderings of the isomers, when compared to both the reference B3PW91/RECP calculations and the B3PW91/def2–TZVPD method. Furthermore, in some cases the B3PW91/LANL2TZ(f) optimizations did not lead to the same minima as the optimizations carried out with the other two methods. Thus, the use of the def2–TZVPD basis is recommended over the LANL2TZ(f) basis set, at least in combination with the B3PW91 density functional.

Conclusions

The structural data and electronic properties obtained using two frequently employed less extensive basis sets for known or novel optimized Au_{10} structures has been assessed against the same parameters obtained with a highly accurate and more extensive energy-consistent scalar-relativistic pseudopotential and basis set. The selected reference method gives results in good agreement with previously published data. The def2–TZVPD basis set and ECP gives relative energies, geometrical parameters and electronic structure data in very good agreement with the reference basis set in conjunction with the same method. Even though the B3PW91/LANL2TZ(f) level of theory gives geometrical parameters, orbital energies, APT charge distributions and other properties in good agreement with the reference calculations, it underestimates relative energy values. In addition different relative energy orderings of the isomers are sometimes found compared with the reference method. Thus, the def2–TZVPD basis set can be successfully employed instead of relativistic pseudopotentials, which are highly accurate but which can be very demanding in terms of computing time and resources.

Acknowledgments This work was supported by Consiliul Național al Cercetării Științifice din Învățământul Superior - Unitatea Executivă pentru Finanțarea Învățământului Superior, a Cercetării, Dezvoltării și Inovării (CNCSIS-UEFISCDI), project PNII–ID_PCCE_129/2008 and the U. S. National Science Foundation (Grant CHE-1057466).

References

1. Assadollahzadeh B, Schwerdtfeger P (2009) J Chem Phys 131:064306–064311
2. De HS, Krishnamurty S, Pal S (2010) J Phys Chem C 114:6690–17285
3. David J, Guerra D, Restrepo A (2012) Chem Phys Lett 539:64–69
4. Choi YC, Kim WY, Lee HM, Kim KS (2009) J Chem Theory Comput 5:1216–1223
5. Pyykkö P (2012) Annu Rev Phys Chem 63:45–64, and references therein
6. Zanti G, Peeters D (2013) Theor Chem Accounts 132:1300
7. Bonacic-Koutecky V, Burda J, Mitric R, Ge M, Zampella G, Fantucci P (2002) J Chem Phys 117:3120–3131
8. Olson RM, Varganov S, Gordon MS, Metiu H, Chretien S, Piecuch P, Kowalski K, Kucharski SA, Musial M (2005) J Am Chem Soc 127:1049–1052
9. Häkkinen H, Moseler M, Landman U (2002) Phys Rev Lett 89: 033401
10. Pyykkö P (2008) Chem Soc Rev 37:1967–1997, and references therein
11. Frisch MJ, Trucks GW, Schlegel HB et al (2009) Gaussian 09 (Revision A.02). Gaussian, Inc, Wallingford
12. Becke AD (1993) J Chem Phys 98:5648–5652
13. Perdew JP (1991) In: Ziesche P, Eschrig HI (eds) Electronic structure of solids. Akademie, Berlin
14. Perdew JP, Chevary JA, Vosko SH, Jackson KA, Pederson MR, Singh DJ, Fiolhais C (1992) Phys Rev B 46:6671–6687

15. Perdew JP, Chevary JA, Vosko SH, Jackson KA, Pederson MR, Singh DJ, Fiolhais C (1993) Phys Rev B 48:4978
16. Perdew JP, Burke K, Wang Y (1996) Phys Rev B 54:16533–16539
17. Neogrády P, Kellö V, Urban M, Sadlej AJ (1997) Int J Quantum Chem 63:557–565
18. Wesendrup R, Hunt T, Schwerdtfeger P (2000) J Chem Phys 112:9356–9362
19. Figgen D, Rauhut G, Dolg M, Stoll H (2005) Chem Phys 311:227–244
20. Peterson KA, Puzzarini C (2005) Theor Chem Accounts 114:283–296
21. King RB, Silaghi-Dumitrescu I, Uță MM (2009) J Phys Chem A 113:527–533
22. Rappoport D, Furche F (2010) J Chem Phys 133:134105–134111
23. Andrae D, Häußermann U, Dolg M, Stoll H, Preuß H (1990) Theor Chem Accounts 77:123–141
24. Hay PJ, Wadt WR (1985) J Chem Phys 82:299–310
25. Roy LE, Hay PJ, Martin RL (2008) J Chem Theory Comput 4:1029–1031
26. Ehlers AW, Böhme M, Dapprich S, Gobbi A, Höllwarth A, Jonas V, Köhler KF, Stegmann R, Veldkamp A, Frenking G (1993) Chem Phys Lett 208:111–114
27. Feller D (1996) J Comput Chem 17:1571–1586
28. Schuchardt KL, Didier BT, Elsethagen T, Sun L, Gurumoorthi V, Chase J, Li J, Windus TL (2007) J Chem Inf Model 47:1045–1052
29. Chen Z, Neukermans S, Wang X, Janssens E, Zhou Z, Silverans RE, King RB, Schleyer PR, Lievens P (2006) J Am Chem Soc 128:12829–12834
30. Sergeeva A, Boldyrev A (2011) J Clust Sci 22:321–329
31. Petrar PM, Sárosi MB, King RB (2012) J Phys Chem Lett 3:3335–3337
32. Li J, Li X, Zhai H-J, Wang L-S (2003) Science 299:864–867
33. Pettersen EF, Goddard TD, Huang CC, Couch GS, Greenblatt DM, Meng EC, Ferrin TE (2004) J Comput Chem 25:1605–1612